

Figure 2. Stereoview of the packing of $P_4(NCH_3)_6CH_3I$ in the unit cell, as viewed along the b axis.

soning that electronegative substituents decrease the size of the d orbitals and allow for more favorable overlap.

The crystal packing consists of sheets of iodide ions lying in the yz plane with $P_4(NCH_3)_6CH_3^+$ cations on each side arranged so that the charged phosphorus atom in each cation points almost directly into the center of a triangle of iodide ions (the distances from this phosphorus to the three nearest iodide ions are 4.57, 4.76, and 4.83 Å). The packing is such that only half of the triangular faces have associated cations. A triangular face of iodide ions is illustrated in the ORTEP drawing of the cation in Figure 1. There are no unusually short intermolecular forces in the molecule.

Acknowledgment. The authors wish to thank the donors

of the Petroleum Research Fund, administered by the American Chemical Society, and the University of Arkansas Research Grant Program.

Registry No. [$P_4(NCH_3)_6CH_3^+][I^-]$, 36919-57-0; $P_4(NCH_3)_6CH_3I$, 51329-59-0.

Supplementary Material Available. A listing of structure factor amplitudes will appear following these pages in the microfilm edition of this volume of the journal. Photocopies of the supplementary material from this paper only or microfiche (105 × 148 mm, 24× reduction, negatives) containing all of the supplementary material for the papers in this issue may be obtained from the Journals Department, American Chemical Society, 1155 16th St., N.W., Washington, D. C. 20036. Remit check or money order for \$3.00 for photocopy or \$2.00 for microfiche, referring to code number INORG-74-1688.

Contribution from the Department of Chemistry, McMaster University, Hamilton, Ontario, Canada

Crystal Structure of $XeF_3^+SbF_6^-$

P. BOLDRINI, R. J. GILLESPIE,* P. R. IRELAND, and G. J. SCHROBILGEN

Received August 22, 1973

AIC30623K

The crystal structure of $XeF_3^+SbF_6^-$ has been accurately determined from three-dimensional X-ray counter data. Crystals are monoclinic with $a = 5.394$ (1) Å, $b = 15.559$ (2) Å, $c = 8.782$ (1) Å, $\beta = 103.10$ (1)°, $V = 717.84$ Å³, $Z = 4$, and $d_c = 3.92$ g cm⁻³. The structure has been refined in space group $P2_1/n$ to a final conventional R factor of 0.048 for 1264 independent reflections with $I \geq 3\sigma(I)$. The structure consists of $XeF_3^+SbF_6^-$ units with a close contact of 2.485 (10) Å between the Xe atom of the T-shaped cation and an F atom of the octahedral anion. The bridging F atom is coplanar with the cation with a bridge angle of 140.8 (4)°.

Introduction

The preparation of the compound $XeF_3^+Sb_2F_{11}^-$ and its characterization by ¹⁹F nmr and Raman spectroscopy was first reported from this laboratory¹ and it was shown that the spectroscopic evidence was in complete accord with the expected T-shape geometry for the XeF_3^+ cation. Subsequently we prepared the crystalline compound $XeF_3^+SbF_6^-$ and had made considerable progress in the determination of its structure by X-ray crystallography when Bartlett, *et al.*, gave a preliminary report² of the structure of $XeF_3^+Sb_2F_{11}^-$. We have since completed the refinement of the structure of $XeF_3^+SbF_6^-$ and we now report the results and compare them in detail with those obtained by Bartlett, *et al.*, for $XeF_3^+Sb_2F_{11}^-$, the full details of which have been published³ since

the completion of our work. At the same time McKee, Adams, and Bartlett⁴ published the unit cell parameters of $XeF_3^+SbF_6^-$.

Experimental Section

Details of the techniques used for the preparation of $XeF_3^+SbF_6^-$ and related complexes are described elsewhere.⁵ The complex was prepared by dissolving XeF_4 and SbF_5 in the ratio 3.4:1 in anhydrous HF. Crystals were grown by slowly pumping the HF off at room temperature, giving a mixture of XeF_4 and $XeF_3^+SbF_6^-$ crystals. Excess XeF_4 was then pumped off at room temperature and pumping continued for several hours to give dry crystals. A Raman spectrum of the single crystal used for the X-ray structure determination showed it to be identical with the bulk material.

Crystal Data. $XeF_3^+SbF_6^-$ is monoclinic with $a = 5.394$ (1) Å, $b = 15.559$ (2) Å, $c = 8.782$ (1) Å, $\beta = 103.10$ (1)°, $V = 717.85$ Å³, $Z = 4$, $d_c = 3.92$ g cm⁻³, $FW = 424.04$, $F(000) = 744$, and $\mu(Mo K\alpha) = 87.6$ cm⁻¹. The unit cell parameters were obtained from a least-squares refinement of 15 reflections in the region $35 < 2\theta < 45^\circ$ and we believe that they are more accurate than those of McKee, Adams,

(1) R. J. Gillespie, B. Landa, and G. J. Schrobilgen, *Chem. Commun.*, 1543 (1971).

(2) D. E. McKee, C. J. Adams, A. Zalkin, and N. Bartlett, *J. Chem. Soc., Chem. Commun.*, 26 (1973).

(3) D. E. McKee, A. Zalkin, and N. Bartlett, *Inorg. Chem.*, 12, 1713 (1973).

(4) D. E. McKee, C. J. Adams, and N. Bartlett, *Inorg. Chem.*, 12, 1722 (1973).

(5) R. J. Gillespie and G. J. Schrobilgen, *Inorg. Chem.*, in press.

and Bartlett.² This is additionally confirmed by the computation of the effective volume per fluorine atom, which is 20 Å and is closer to the values suggested by Zachariasen⁶ and by Edwards and Sills.⁷ Preliminary precession photographs revealed systematic absences: $h0l, h+1=2n+1; 0k0, K=2n+1$. These unambiguously indicated the space group $P2_1/n$, an alternative orientation of $P2_1/c$; equivalent positions for the nonstandard setting are $x, y, z; x, y, z; 1/2-x, 1/2+y, 1/2-z; 1/2+x, 1/2-y, 1/2+z$.⁸

X-Ray Measurements. A needle-shaped crystal with approximate dimensions $0.12 \times 0.14 \times 0.48$ mm, sealed in a quartz capillary, was examined on a Syntex \overline{PI} diffractometer equipped with a fine-focus Mo anode tube and graphite monochromator ($\lambda(\text{Mo } K\alpha) 0.71069$ Å). The crystal was mounted with c^* coincident with ψ of the diffractometer. Intensity data were collected by the $\theta-2\theta$ scan technique, with scan rates varying from 2.0 to 24.0°/min (in 2θ) so that the weaker reflections were examined most slowly to minimize counting errors. Stationary-background counts, with a time equal to half the scan time for each reflection, were made at each end of the scan range. The scan width varied from 2° at low 2θ to 2.5° for the higher angle data. Two standards were checked every 50 reflections to monitor the stability of the crystal and its alignment. The intensities of these standards dropped regularly to about 90% of their original values during the course of the data collection; this decomposition was later corrected for by scaling the data linearly between each set of standards. A total of 2430 reflections within a unique quadrant with $2\theta < 65^\circ$ were measured, resulting in 1264 reflections with intensities greater than 3 times their standard deviation based on counting statistics. Lorentz and polarization corrections were applied to these observed data. The absorption correction was computed with $\mu R = 0.6$, assuming the crystal to be cylindrical.

Solution and Refinement of the Structure. The positions of the heavy atoms were readily located from inspection of the three-dimensional Patterson function. Both atoms were assigned xenon scattering factors, and full-matrix least-squares refinement of positional and isotropic temperature parameters gave a conventional agreement index $R_1, R_1 = \Sigma \Delta / \Sigma |F_o|$ where $\Delta = |F_o| - |F_c|$, of 0.20. Resulting temperature factor differences indicated the probable antimony atom. A difference Fourier synthesis revealed the remaining nine fluorine atoms and confirmed the choice of the antimony atom by the stereochemistry about the two refined heavy atoms. Refinement of positional and anisotropic temperature parameters for all atoms converged at $R_1 = 0.054$, while the weighted agreement index $R_2, R_2 = (\Sigma w \Delta^2 / \Sigma w F_o^2)^{1/2}$ was 0.061 with unit weights. An isotropic correction for secondary extinction was now included in the computations. One further cycle of refinement, using weights inversely proportional to the variances of the intensities, lowered R_1 to 4.8%. Careful examination at this point of all the observed and calculated structure factors showed that the distribution of $\Delta(F_o - F_c)^2$ was, as usual, spread over the F_o^2 and $(\sin \theta) / \lambda$ ranges. For the final cycle therefore a simplified empirical weighting scheme was applied: $\sqrt{w} = (A + BF_o)^{-1}$ with $A = 137.35$ and $B = 0.16$. Using these weights the final agreement factors are $R_1 = 4.8, R_2 = 5.8$, and $R_3 = 7.8$, where R_3 is the agreement of the 390 reflections with observed intensities smaller than 3 times their standard deviation. The applied correction for extinction, as defined in the XRAY-71 system,⁹ amounted to $g = 0.954 \times 10^{-4}$. In the last cycle the largest shift of any parameter divided by its estimated standard deviation was 0.46, while the standard deviation of an observation of unit weight was 0.019. These facts, together with the remarkably low agreement factor for the weak reflections, indicated that the refinement was successfully completed and the collected data were of good quality. The final difference Fourier was featureless except for four small positive peaks within 1 Å of the heavy atoms. The atomic scattering factors used, with anomalous dispersion corrections for Xe and Sb, were the well-known values of Cromer.¹⁰

All calculations were performed on a CDC 6400 computer using the series of programs in the XRAY-71 system⁹ and our own programs. The final atomic positional coordinates and temperature factors are given in Table I. A tabulation of structure amplitudes is available.¹¹

(6) W. H. Zachariasen, *J. Amer. Chem. Soc.*, **70**, 2147 (1948).

(7) A. J. Edwards and R. J. C. Sills, *J. Chem. Soc. A*, 942 (1971).

(8) "International Tables for X-Ray Crystallography," Vol. 1, Kynoch Press, Birmingham, England, 1962.

(9) J. M. Stewart, F. A. Kundell, and J. C. Baldwin, "XRAY 71 System of Crystallographic Programs," Technical Report, University of Maryland, 1971.

(10) D. T. Cromer and J. R. Mann, *Acta Crystallogr., Sect. A*, **24**, 321 (1968); D. T. Cromer, *Acta Crystallogr.*, **18**, 17 (1965).

(11) See paragraph at end of paper regarding supplementary material.

Description and Discussion of the Structure

Figure 1 shows the configuration of the $\text{XeF}_3^+\text{SbF}_6^-$ unit, while Table II lists interatomic distances and angles. Packing of the units is illustrated in Figure 2.

The XeF_3^+ cation has the planar T shape expected for an AX_3E_2 molecule, *i.e.*, a molecule in which there is a trigonal-bipyramidal arrangement of five electron pairs in the valence shell of the central atom. Two of the electron pairs are non-bonding and, as in all molecules of this type, occupy equatorial positions in order to minimize their interactions with the bonding electron pairs.¹² The axial bonds are longer than the equatorial bond owing to the greater repulsive interaction between the axial bonding electron pairs and their neighbors.¹² The presence of the large lone pairs also diminishes the bond angles from the ideal value of 90°. Similar structural features have been found for the electronically related BrF_3 ^{13,14} and ClF_3 ¹⁵ molecules (Table III). Our structural parameters for XeF_3^+ are in good agreement with those obtained by Bartlett, *et al.*³ (Table III).

There is a short contact of 2.49 Å between F(1) of the SbF_6^- anion and the XeF_3^+ cation, and the direction of the interaction is of considerable interest. This fourth fluorine atom in the neighborhood of the xenon is coplanar with the other three fluorine atoms and the xenon atom (Table IV). This interaction is best described as a weak covalent bond formed by the donation of a formally unshared electron pair on the fluorine to the xenon. The direction of this interaction is dictated by the tendency for the incoming electron pair of F(1) to avoid the other electron pairs in the valency shell of xenon and, accordingly, is expected to be directed toward the middle of one of the triangular faces of the trigonal bipyramid as shown in Figure 3. It is interesting to note that if the arrangement of electron pairs around xenon is assumed to be a regular trigonal bipyramid with dimensions given by the observed Xe-F bond distances, then the angle subtended by the Xe-F(3) bond and another fluorine approaching the midpoint of one of the faces containing the two lone pairs is 151°. This value is remarkably close to the observed angle of 153° for F(1)-Xe-F(3).

There is also a relatively short intermolecular contact of 2.71 Å between the F(7) of one $\text{XeF}_3^+\text{SbF}_6^-$ unit and the xenon of an adjacent unit with two such interactions linking pairs of $\text{XeF}_3^+\text{SbF}_6^-$ units into dimers (Figure 2). This interaction may also be regarded as a weak covalent bond due to a partial donation of a pair of electrons of F(7) into the valence shell of the xenon. The direction of this interaction also appears to be very significant as it is directed toward the center of the second face of the trigonal bipyramid containing the two lone pairs and makes an angle with the Xe-F(3) bond of 143° which is again quite close to the "ideal" value of 151° (Figure 3). Moreover, F(7) is also coplanar with F(1), F(2), F(3), and F(4) (Table IV), forming, together with the two axial Xe-F bonds, the equatorial Xe-F bond, the Xe-F bridge bond, and the two lone pairs, an approximate pentagonal-bipyramidal arrangement of seven electron pairs around the xenon. The lone pairs of xenon are in the axial positions as would be anticipated in view of their larger interactions with other electron pairs.¹² The planarity of the bonds around xenon is analytically well defined and it

(12) R. J. Gillespie, "Molecular Geometry," Van Nostrand-Reinhold, London, 1972.

(13) D. F. Smith, *J. Chem. Phys.*, **21**, 609 (1953).

(14) R. D. Burbank and F. N. Bensey, *J. Chem. Phys.*, **21**, 602 (1953).

(15) D. W. Magnuson, *J. Chem. Phys.*, **27**, 223 (1957).

Table I. Positional and Thermal Parameters U_{ij} for $\text{XeF}_3^+\text{SbF}_6^-$

	<i>x</i>	<i>y</i>	<i>z</i>	U_{11}	U_{22}	U_{33}	U_{12}	U_{13}	U_{23}
Xe	0.11863 (19)	0.13972 (5)	0.21679 (10)	0.0509 (6)	0.0270 (4)	0.0280 (4)	0.0030 (4)	0.0170 (3)	0.0036 (3)
Sb	-0.26927 (19)	-0.08283 (6)	0.27876 (10)	0.0350 (5)	0.0277 (4)	0.0262 (4)	-0.0007 (4)	0.0082 (3)	0.0044 (3)
F(1)	-0.1023 (17)	0.0249 (5)	0.3317 (9)	0.046 (5)	0.038 (4)	0.038 (4)	-0.012 (4)	0.005 (4)	0.001 (4)
F(2)	-0.2176 (22)	0.1323 (8)	0.0891 (12)	0.059 (7)	0.082 (8)	0.046 (5)	0.002 (6)	-0.002 (5)	0.010 (5)
F(3)	0.1409 (24)	0.2196 (6)	0.0669 (10)	0.111 (9)	0.036 (5)	0.033 (4)	0.001 (5)	0.026 (5)	0.011 (4)
F(4)	0.4629 (23)	0.1749 (8)	0.2930 (13)	0.069 (8)	0.076 (8)	0.055 (6)	0.028 (6)	0.015 (6)	0.006 (5)
F(5)	-0.2120 (21)	-0.0672 (7)	0.0785 (11)	0.074 (7)	0.063 (6)	0.039 (5)	-0.012 (5)	0.037 (5)	-0.006 (4)
F(6)	-0.4294 (19)	-0.1873 (6)	0.2209 (11)	0.065 (7)	0.034 (4)	0.051 (5)	-0.016 (4)	0.006 (5)	0.002 (4)
F(7)	-0.3229 (19)	-0.0928 (7)	0.4831 (9)	0.053 (6)	0.080 (7)	0.024 (4)	-0.015 (5)	0.003 (4)	0.014 (4)
F(8)	-0.5742 (19)	-0.0222 (6)	0.2273 (11)	0.053 (6)	0.055 (6)	0.046 (5)	0.016 (5)	0.006 (4)	0.002 (5)
F(9)	0.0376 (24)	-0.1366 (8)	0.3455 (18)	0.053 (8)	0.063 (7)	0.128 (114)	0.024 (6)	0.022 (7)	0.021 (8)

Table II. Interatomic Distances (Å) and Angles (deg) for $\text{XeF}_3^+\text{SbF}_6^-$ ^a

Xe-F(1)	2.485 (10)	F(2)-F(3)	2.41	Xe-F(1)-Sb	140.8 (4)
-F(2)	1.907 (15)	-F(5)	2.83	F(1)-Xe-F(2)	73.5 (4)
-F(3)	1.835 (10)	-F(6)	3.07	-F(3)	153.4 (4)
-F(4)	1.906 (13)	F(3)-F(4)	2.43	-F(4)	125.6 (4)
Sb-F(1)	1.910 (9)	-F(5)	2.76	F(2)-Xe-F(3)	80.1 (5)
-F(5)	1.869 (11)	-F(6)	2.80	-F(4)	160.9 (5)
-F(6)	1.857 (10)	-F(9)	2.83	F(3)-Xe-F(4)	80.8 (4)
-F(7)	1.888 (10)	-F(4)'	2.89	F(1)-Sb-F(5)	86.9 (4)
-F(8)	1.861 (11)	-F(6)'	3.29	-F(6)	178.2 (4)
-F(9)	1.829 (14)	F(4)-F(7)	2.60	-F(7)	90.3 (4)
Xe-F(7)	2.715 (13)	-F(8)	3.12	-F(8)	87.5 (4)
-F(5)	2.974 (11)	F(5)-F(9)	2.65	-F(9)	88.9 (5)
-F(6)	2.973 (10)	-F(6)	2.66	F(5)-Sb-F(6)	91.2 (5)
-F(8)	3.006 (10)	-F(8)	2.68	-F(7)	177.2 (5)
F(1)-F(5)	2.60	-F(8)'	3.01	-F(8)	91.8 (5)
-F(8)	2.61	F(6)-F(9)	2.63	-F(9)	91.7 (6)
-F(9)	2.62	-F(7)	2.68	F(6)-Sb-F(7)	91.5 (5)
-F(2)	2.67	-F(8)	2.69	-F(8)	92.7 (4)
-F(7)	2.69	-F(2)'	3.07	-F(9)	91.0 (5)
-F(7)'	2.71	F(7)-F(8)	2.59	F(7)-Sb-F(8)	87.4 (4)
-F(1)'	3.01	-F(9)	2.60	-F(9)	88.9 (6)
		-F(3)'	3.36	F(8)-Sb-F(9)	174.8 (6)

^a A prime notation indicates an atom in a symmetry-related position. The standard deviation of the F-F distance is 0.015 Å.

Table III. Comparison of the Structures of XeF_3^+ , BrF_3 , and ClF_3

	$\text{XeF}_3^+\text{SbF}_6^-$	$\text{XeF}_3^+\text{Sb}_2\text{F}_{11}^-$	BrF_3	ClF_3
X-F _{eq} , Å	1.84	1.83	1.721	1.598
X-F _{ax} , Å	1.91	1.88, 1.89	1.810	1.698
X-F _{br} , Å	2.49	2.50		
F _{ax} -X-F _{eq} , deg	81, 80	82, 80	86.2	87.5
F _{eq} -X-F _{br} , deg	141	172		
Ref	This work	3	13, 14	15

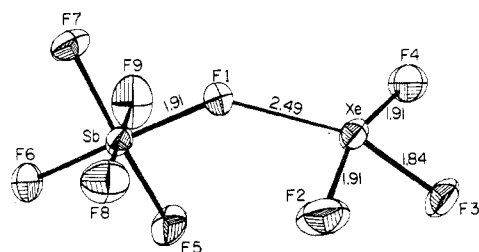


Figure 1. A perspective view of the $\text{XeF}_3^+\text{SbF}_6^-$ structural unit with the atoms as 50% probability thermal ellipsoids. Interatomic distances are in angstroms.

appears to be a characteristic of the cation (Table IV) as it is found in both $\text{XeF}_3^+\text{SbF}_6^-$ and $\text{XeF}_3^+\text{Sb}_2\text{F}_{11}^-$.³

The bridging Sb-F(1) distance of 1.914 (7) Å is significantly longer than the bond distances to the other fluorine atoms of the approximately octahedral SbF_6^- anion. The increased length of this bond arises from the greater polarity imparted

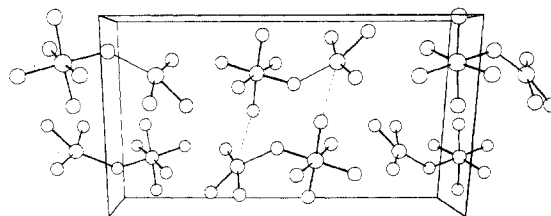


Figure 2. A perspective illustration of the packing of the $\text{XeF}_3^+\text{SbF}_6^-$ units within the unit cell as viewed down the *a* axis. The dotted lines show the close approach between the Xe and neighboring F atoms.

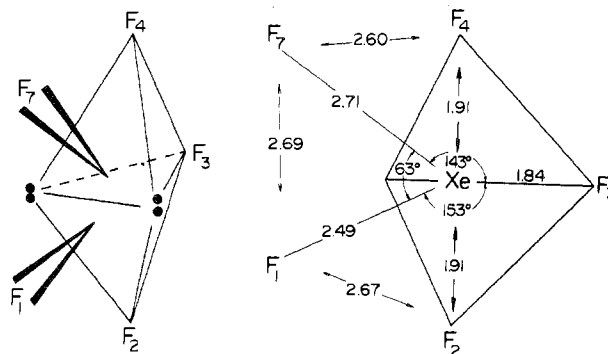


Figure 3. An approximate model for the fluorine bridging in $\text{XeF}_3^+\text{SbF}_6^-$.

Table IV. Equations for Least-Squares Planes^a

Atoms in the plane	A	B	C	D	$\sigma(A)$	χ^2	ν	Remarks
F(2), F(3), F(4) ^b	-2.358X + 11.097Y + 5.556Z = 2.477				0	0	2	Xe is -0.002 Å out of this plane
XeF_3^+ ^b	-2.359X + 11.091Y + 5.559Z = 2.476				0.001	0.02	3	F(1) is -0.113 Å out of this plane; F(7) is -0.058 Å out of this plane
$\text{XeF}_3^+ \cdots \text{F}(1)^b$	-2.410X + 10.768Y + 5.738Z = 2.440				0.024	25.22	4	This LS plane forms an angle of 1.69° with the LS plane of XeF_3^+
$\text{XeF}_3^+ \cdots \text{F}(7)^b$	-2.376X + 10.987Y + 5.618Z = 2.466				0.007	2.12	4	This LS plane forms an angle of 0.55° with the LS plane of XeF_3^+ and an angle of 1.14° with the LS plane of $\text{XeF}_3^+ \cdots \text{F}(1)$
$\text{XeF}_3^+ \cdots \text{F}(7)^b$ $\cdots \text{F}(1)$	-2.383X + 10.939Y + 5.646Z = 2.453				0.033	57.95	5	
XeF_3^+ ^c	-6.683X + 6.708Y + 6.316Z = 4.236				0.012	2.12	3	Xe is 0.026 Å out of this plane
$\text{XeF}_3^+ \cdots \text{F}(2)^c$	-6.679X + 6.753Y + 6.332Z = 4.217				0.011	2.51	4	This LS plane forms an angle of 0.2° with the previous one

^a Equations defined by $AX + BY + CZ = D$ in direct crystal coordinate system. σ is the standard deviation; χ^2 expresses the statistical probability of the LS (least-squares) plane, and ν represents the degrees of freedom of the statistical distribution. ^b $\text{XeF}_3^+\text{SbF}_6^-$; present work. ^c $\text{XeF}_3^+\text{Sb}_2\text{F}_{11}^-$, ref 3.

by the greater effective electronegativity of the bridging fluorine, F(1). This, in turn, is due to the partial donation of one of the formally nonbonding pairs of F(1) to the xenon atom. The greater polarity of the Sb-F(1) bond implies that this bond has a smaller repulsive interaction with the neighboring Sb-F bonds¹² and, consequently, all the F(1)-Sb-F angles are smaller than the corresponding F(6)-Sb-F angles by an average of 3.5°. It is noteworthy that even the second very weak interaction involving F(7) appears to cause some further distortion of the SbF_6^- anion. Thus the Sb-F(7) bond is the second longest after the Sb-F(1) bond, the adjacent angle F(7)-Sb-F(8) is slightly smaller than 90°, and the angles F(5)-Sb-F(8) and F(5)-Sb-F(9) are both slightly larger than 90°.

All three Xe-F bonds in XeF_3^+ are significantly shorter than the Xe-F bond distance of 1.95 Å in XeF_4 . This is consistent with a decreased bond polarity resulting from the increased effective electronegativity of the xenon produced by its formal positive charge. Similar decreases in bond length have been observed on going from XeF_2 to XeF^+ and from XeF_6 to XeF_5^+ .¹⁶ Our explanation for these bond shortenings differs from that given by Bartlett, *et al.*^{3,17} These authors claim that this shortening is due to an increased bond polarity consequent upon an increased effective nuclear charge on xenon. Since, however, the bond is polar in the sense $\text{Xe}^{\delta+} \delta^- \text{F}$ an increased positive charge on xenon which increases its effective electronegativity can only reduce this bond polarity. This decreased bond polarity in turn increases the strength and decreases the length of the bond.

Bartlett, *et al.*,³ accounted for the difference in the axial and equatorial bond lengths of XeF_3^+ in terms of the Pimentel-Rundle model^{18,19} in which the axial bonds are formulated as three-center four-electron bonds with a bond order of one-half and the equatorial bond is regarded as a normal electron pair bond with a bond order of unity. The relatively small difference in the axial and equatorial bond lengths does not, however, seem to be consistent with the rather large difference in bond order predicted by this theory. The difference in the axial and equatorial bond lengths decreases in the series ClF_3 , BrF_3 , XeF_3^+ (Table III), in the reverse order of that expected on the basis of the three-center four-electron bond

theory which predicts a greater difference as the lengths of both bonds increase. This diminishing difference between the axial and equatorial bond lengths is, however, in agreement with the idea that the geometry of these AX_3E_2 molecules is primarily determined by the interactions of bonding and nonbonding electron pairs in the valence shell of the central atom. These interactions diminish with increasing size of the valency shell in the series Cl, Br, Xe, and as it is these interactions that are responsible for the difference in the axial and equatorial bond lengths, this difference also decreases accordingly. Bartlett, *et al.*,³ also gave an explanation along these lines although it is inconsistent with their basic assumption of three-center four-electron bonding. However, they preferred to speak of interactions between the ligands and the lone-pair electrons, whereas the electron pair repulsion model is based on the fundamental idea that it is the interactions between bonding and nonbonding electron pairs in the valency shell that are responsible for molecular geometry. According to this model, ligand-ligand interactions (*i.e.*, interactions between the nonbonding electron pairs on the ligands) are generally less important than bond-bond and bond-lone pair interactions. It should also be noted that on the basis of the three-center four-electron bond theory, Bartlett²⁰ has considered the bonds in XeF_2 , which have a length of 2.00 Å,²¹ to be half-bonds and the bond in XeF^+ , which has a length of 1.84 Å in $\text{XeF}^+\text{Sb}_2\text{F}_{11}^-$, to be a full bond. The difference of 0.16 Å is much greater than that between the axial and equatorial bonds of XeF_3^+ .

The decreasing bond angles in the series ClF_3 , BrF_3 , XeF_3^+ find no explanation in terms of the three-center four-electron bond theory. The trend can be understood as a direct consequence of the increased size of the valency shell which allows the bonding electron pairs to subtend a smaller angle at the nucleus of xenon under the repulsive interaction of the lone pairs before they begin to interact appreciably. However, it must be admitted that the formation of the bridge bonds will also tend to reduce the F-Xe-F angles so comparison of bond angles in the series ClF_3 , BrF_3 , and XeF_3^+ is perhaps not entirely justified.

The most striking difference between the structure of $\text{XeF}_6^+\text{SbF}_6^-$ and that of $\text{XeF}_3^+\text{Sb}_2\text{F}_{11}^-$ is the difference in the bridge bond angle in the present structure (140.8°) and in the 1:2 structure (171.6°). This cannot be attributed to the difference in the anions because in $\text{XeF}^+\text{Sb}_2\text{F}_{11}^-$ the bridging

(16) F. Sladky, *MTP (Med. Tech. Publ. Co.) Int. Rev. Sci.: Inorg. Chem., Ser. One*, 3, 1 (1972).

(17) N. Bartlett, M. Gennis, D. D. Gibling, B. K. Morrell, and A. Zalkin, *Inorg. Chem.*, 12, 1717 (1973).

(18) G. C. Pimentel, *J. Chem. Phys.*, 19, 446 (1951).

(19) R. E. Rundle, *J. Amer. Chem. Soc.*, 85, 112 (1963).

(20) N. Bartlett, *Endeavour*, 31, 107 (1972).

(21) V. M. McRae, R. D. Peacock, and D. R. Russell, *Chem. Commun.*, 62 (1969).

angle is 147° .³ It would seem that this angle is rather easily distorted by packing considerations and that its exact value is perhaps not highly significant. It is perhaps influenced by the intermolecular contact Xe-F(7) which is not present in the $\text{XeF}_3^+\text{Sb}_2\text{F}_{11}^-$ structure.

We conclude that the structure of $\text{XeF}_3^+\text{SbF}_6^-$ is essentially ionic, but that there is a weak covalent interaction between the two ions by a fluorine bridge and that both the ions are slightly distorted by this interaction. In particular, the Sb-F(1) bond that is involved in this bridging interaction is slightly longer than the other Sb-F bonds and there is a corresponding distortion of the bond angles from the ideal angle of 90° . There are also two weak intermolecular interactions between pairs of $\text{XeF}_3^+\text{SbF}_6^-$ units which thus form cyclic dimers. The directions of these interactions again indicate that they may be regarded as weak covalent bonds. The similarity of all the parameters of XeF_3^+ , including the Sb-F-

Xe bridging distances, in both the SbF_6^- and $\text{Sb}_2\text{F}_{11}^-$ compounds (Table III) implies that there is an almost identical interaction between the SbF_6^- and $\text{Sb}_2\text{F}_{11}^-$ anions and the XeF_3^+ cation.

Acknowledgments. We thank the National Research Council of Canada for financial support of this work and for a scholarship to G. J. S.

Registry No. $\text{XeF}_3^+\text{SbF}_6^-$, 39797-63-2.

Supplementary Material Available. A listing of structure factor amplitudes will appear following these pages in the microfilm edition of this volume of the journal. Photocopies of the supplementary material from this paper only or microfiche (105×148 mm, $24\times$ reduction, negatives) containing all of the supplementary material for the papers in this issue may be obtained from the Journals Department, American Chemical Society, 1155 16th St., N.W., Washington, D. C. 20036. Remit check or money order for \$3.00 for photocopy or \$2.00 for microfiche, referring to code number INORG-74-1690.

Contribution from the Department of Chemistry,
McMaster University, Hamilton, Ontario L8S 4M1, Canada

Fluorine-19 Nuclear Magnetic Resonance and Raman Spectroscopic Study of the $(\text{FXe})_2\text{SO}_3\text{F}^+$ Cation. Preparation and Characterization of $(\text{FXe})_2\text{SO}_3\text{F}^+\text{AsF}_6^-$

R. J. GILLESPIE* and G. J. SCHROBILGEN

Received October 4, 1973

AIC30723Q

The reaction of the Xe_2F_3^+ cation with HSO_3F has been studied in solution by ^{19}F nmr spectroscopy and shown to give rise to the cation $(\text{FXe})_2\text{SO}_3\text{F}^+$. The compound $(\text{FXe})_2\text{SO}_3\text{F}^+\text{AsF}_6^-$ has also been prepared and studied in BrF_3 solution by ^{19}F nmr and in the solid phase by Raman spectroscopy. The cation is shown to contain the fluorosulfate group in the bridging position.

Introduction

A number of xenon(II) compounds have been prepared by substitution of a highly electronegative ligand for one or both of the fluorines in xenon difluoride.¹⁻⁸ The fluorine-bridged cations Xe_2F_3^+ ^{9,10} and Kr_2F_3^+ ¹¹ are now well-established species both in the solid phase and in solution. It was therefore of interest to determine if electronegative groups other than fluoride could also form similar bridged species. We describe in this paper the preparation and characterization by ^{19}F nmr and Raman spectroscopy of the fluorosulfate-bridged cation $(\text{FXe})_2\text{SO}_3\text{F}^+$. We have previously given a preliminary report of the ^{19}F nmr parameters of this ion¹² and Bartlett and coworkers⁸ have reported on an independent

preparation of $(\text{FXe})_2\text{SO}_3\text{F}^+\text{AsF}_6^-$ and its Raman spectrum. The present work which includes a more detailed analysis of the Raman spectrum of $(\text{FXe})_2\text{SO}_3\text{F}^+\text{AsF}_6^-$ than reported previously as well as a detailed ^{19}F nmr investigation of the formation and decomposition of the $(\text{FXe})_2\text{SO}_3\text{F}^+$ cation in HSO_3F solution proves that the SO_3F group is indeed situated in the bridging position.

Results and Discussion

^{19}F Nmr Spectroscopy. In an attempt to obtain the ^{19}F nmr spectrum of Xe_2F_3^+ from solutions of the compounds $\text{Xe}_2\text{F}_3^+\text{SbF}_6^-$ and $\text{Xe}_2\text{F}_3^+\text{AsF}_6^-$ in HSO_3F , it was found that the spectrum changed with time and apparently several species were formed. It was evident that Xe_2F_3^+ undergoes a reaction in fluorosulfuric acid although its spectrum can be obtained in BrF_3 solution in which it is stable.¹⁰

If the ^{19}F nmr spectrum of either compound in HSO_3F solution is measured at -95° , immediately after its preparation at approximately -40° , it shows a high-field peak, A, accompanied by ^{129}Xe satellites (Figure 1a and Table I). This peak cannot be assigned to XeF_2 , FXeSO_3F , or Xe_2F_3^+ ¹⁰ and must be due to a new species which we propose to be $(\text{FXe})_2\text{SO}_3\text{F}^+$. On the basis of its chemical shift and the absence of a ^{129}Xe - ^{19}F coupling constant, a second high-field peak, B, may be assigned to HF. These assignments are supported by the observation of a peak, A', in the F-on-S region of the spectrum in addition to that due to the solvent. The integrated relative intensities of the MF_6^- (C), HF, and F-on-Xe environments were 6:1:2, respectively. Unfortunately, the

(1) N. Bartlett, M. Wechsberg, F. O. Sladky, P. A. Bulliner, G. R. Jones, and R. D. Burbank, *Chem. Commun.*, 703 (1969).

(2) N. Bartlett, M. Wechsberg, G. R. Jones, and R. D. Burbank, *Inorg. Chem.*, 11, 1124 (1972).

(3) F. Sladky, *Monatsh. Chem.*, 101, 1559 (1970).

(4) F. Sladky, *Monatsh. Chem.*, 101, 1571 (1970).

(5) F. Sladky, *Monatsh. Chem.*, 101, 1578 (1970).

(6) K. Seppelt, *Angew. Chem., Int. Ed. Engl.*, 11, 723 (1972).

(7) M. Eisenberg and D. D. Des Marteau, *Inorg. Chem.*, 11, 1901 (1972).

(8) M. Wechsberg, P. A. Bulliner, F. O. Sladky, R. Mews, and N. Bartlett, *Inorg. Chem.*, 11, 3063 (1972).

(9) F. O. Sladky, P. A. Bulliner, N. Bartlett, B. G. De Boer, and A. Zalkin, *Chem. Commun.*, 1048 (1968).

(10) R. J. Gillespie, A. Netzer, and G. J. Schrobilgen, *Inorg. Chem.*, 13, 1455 (1974).

(11) R. J. Gillespie and G. J. Schrobilgen, *J. Chem. Soc., Chem. Commun.*, 90 (1974).

(12) R. J. Gillespie, paper presented at the First Winter Fluorine Conference, St. Petersburg, Fla., Jan 24-28, 1972.